International Core Journal of Engineering Volume 10 Issue 5, 2024
ISSN: 2414-1895 DOI: 10.6919/ICJE.202405_10(5).0065

# Structural Enhancement and Experimental Validation of a Horizontal Single-Tube Heat Transfer Test Bench

Haowei Sun

School of Environment and Architecture, University of Shanghai For Science and Technology, Shanghai, China

## Abstract

**In order to maintain measurement accuracy while minimizing testing time, an enhanced horizontal single tube heat transfer performance testing device is proposed. The improved device utilizes R134a as a refrigerant for full liquid evaporation, external condensation, and falling film evaporation experiments. Explained the system principles and processes. Validation and repeatability testing were conducted on the evaporation and condensation of the lamp tube. An error analysis was conducted on the measured and theoretical heat transfer coefficients, and the results were compared with those of the original experimental platform. The research results indicate that under the same conditions, the accuracy of the new setting has increased by 3% and the testing time has been shortened by 5 hours. This platform significantly simplifies the experimental procedures while maintaining accuracy, providing a simplified structure and reduced steps.**

## Keywords

**Falling Film Evaporation; Horizontal Single-Tube; R134a; Heat Transfer Coefficient.**

## 1. Introduction

The horizontal single-tube heat transfer performance test bench serves as experimental apparatus for assessing the heat transfer efficacy of liquids or gases within a single tube. By regulating the temperature differential between the heater and cooler, it induces heat transfer phenomena. Typically crafted from high thermal conductivity materials, the single tube ensures rapid heat transfer to the medium. Equipped with sensors and a data acquisition system, the bench monitors and records parameters such as temperature, pressure, and flow rate within the tube, facilitating the computation of crucial metrics like heat transfer coefficient and thermal resistance. Building upon theoretical foundations and prior experimental insights[1], the author enhanced the experimental setup by modifying the refrigerant circulation path during full liquid evaporation and external condensation experiments. Comparative analyses were conducted under identical conditions, demonstrating the improved efficiency of the experimental configuration in reducing testing duration while maintaining result accuracy.

## 2. Testing System and Experimental Principles

### 2.1 Test System Composition

The experimental setup comprises essential components such as an evaporator, falling film evaporator, auxiliary condenser, ethylene glycol water tank, constant temperature water tank, refrigeration unit, spray pipe, flow meter, water pump, refrigerant storage tank, constant temperature water tank electric heater, and associated system accessories. The schematic diagram illustrating the experimental configuration is depicted in Figure 1. Through precise control of pipelines and valves and

ISSN: 2414-1895 DOI: 10.6919/ICJE.202405_10(5).0065

manipulation of the refrigerant circulation path, this device facilitates three distinct test conditions: full liquid evaporation, external condensation, and external falling film evaporation.

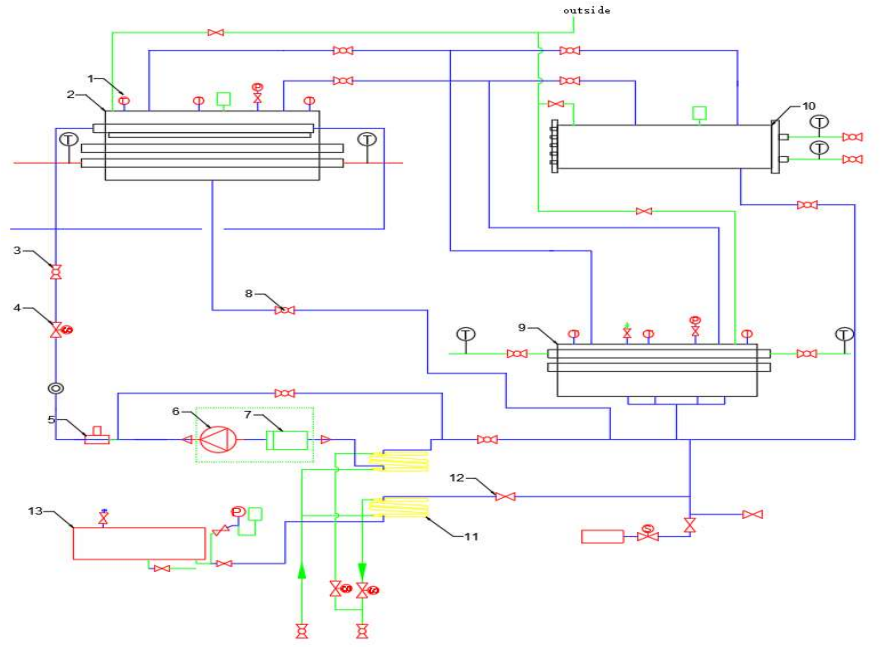


**Figure 1.** Testing System Schematic - Refrigerant Section

1.Platinum resistance thermometer 2.Falling film evaporation/external condensation test bucket 3.ball valve 4.solenoid valve 5.Refrigerant flow meter 6.Refrigerant circulation pump 7.Subcooling controller 8.Bypass valve 9.Full liquid evaporation test bucket 10.Auxiliary condenser drum 11.Subcooling coil 12.Refrigeration system shut-off valve 13.Refrigerant storage tank

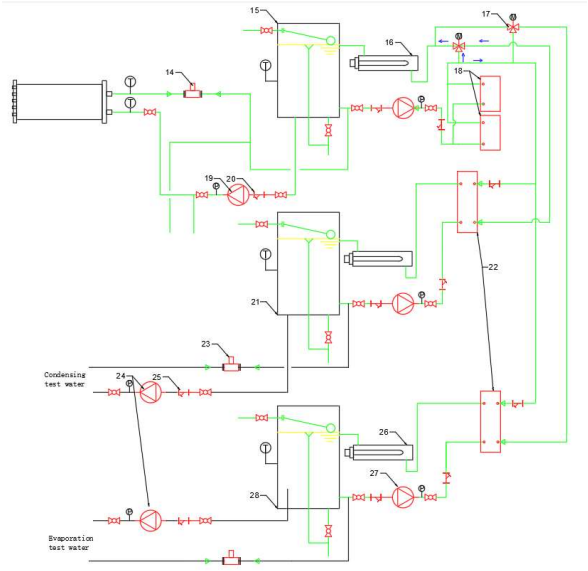


**Figure 2.** Testing System Schematic - Water Section

14.Ethylene glycol flow meter 15.Ethylene glycol water tank 16.Ethylene glycol electric heating 17.Three way regulating valve 18.Refrigeration unit 19.Ethylene glycol testing pump 20.Ethylene Glycol Impurity Filter 21.Condensation test constant temperature water tank 22.Plate heat exchanger 23.Condensation test water flow meter 24.Test water pump 25.Test water filter 26.Testing water electricity heating 27.Circulating water pump 28.Evaporation test constant temperature water tank

ISSN: 2414-1895 DOI: 10.6919/ICJE.202405_10(5).0065

## 2.2 Exprimental Principles

### 2.2.1 Full Liquid Evaporation

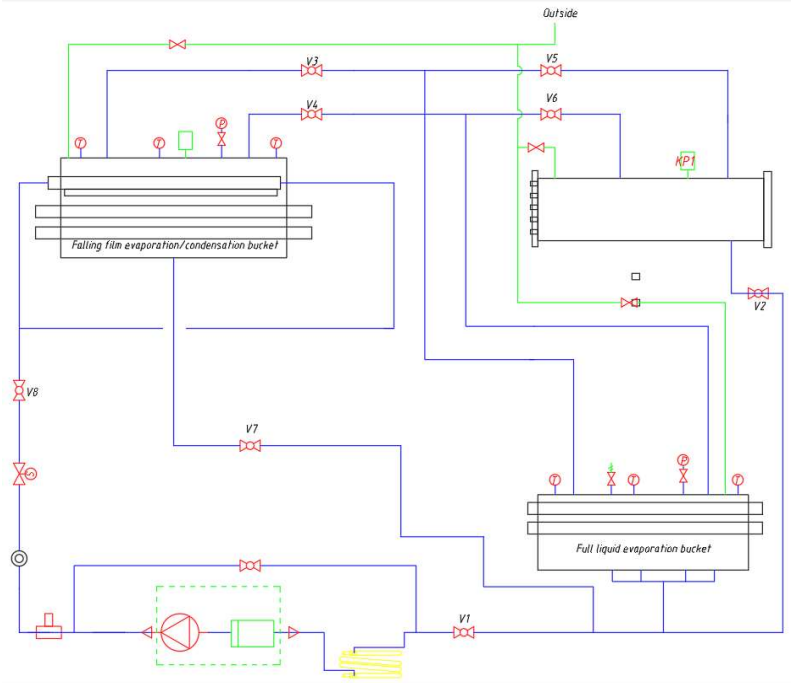


**Figure 3.** Testing System Schematic - Water Section

In the full-liquid evaporation scenario, the operational principle of the refrigerant circulation system is illustrated in Figure 3. By closing gas valves V3 and V4, along with liquid valves V1 and V7, the setup ensures precise control. The refrigerant liquid level is maintained approximately 2-3 cm above the height of the test copper tube within the full-liquid evaporation drum, guaranteeing complete submersion. Within this drum, the liquid refrigerant absorbs thermal energy from the hot water contained within the test copper tube, undergoing evaporation into a gaseous state. Subsequently, the gaseous refrigerant is directed via gas valves V5 and V6 to the auxiliary condensation drum. Here, it transfers heat to a 60% ethylene glycol solution, facilitating its condensation back into a liquid state. The condensed refrigerant then proceeds through liquid valve V2, returning to the full-liquid evaporation drum to complete the refrigerant cycle.

### 2.2.2 Falling Film Evaporation

In the operational phase of falling film evaporation, the liquid refrigerant is uniformly dispersed onto the test copper tube within the falling film chamber via the spraying mechanism. Here, it absorbs the thermal energy emitted by the hot water flowing within the copper tube, undergoing a phase change into gaseous refrigerant. Any residual liquid refrigerant not yet evaporated is directed back to the full liquid evaporation chamber through the liquid valve V7. Meanwhile, the evaporated gaseous refrigerant is conveyed to the auxiliary condensation chamber through the gas valves V5 and V6. Upon entering this chamber, the gaseous refrigerant relinquishes its heat to the ethylene glycol solution, thus transitioning back into a liquid state. Subsequently, the condensed refrigerant flows back to the full liquid evaporation chamber through the liquid valve V2. Here, it is propelled into the spray pipe by the refrigerant circulation pump via the liquid valve V1, effectively completing a single refrigerant cycle.

### 2.2.3 External Condensation

In the external condensation phase, the operational adjustments involve the closure of liquid valves V1 and V2, along with air valves V5 and V6, while the opening of air valves V3, V4, and liquid valves V7 is enacted. Herein, the liquid refrigerant undergoes a phase change, absorbing thermal

ISSN: 2414-1895 DOI: 10.6919/ICJE.202405_10(5).0065

energy from the hot water contained within the full liquid evaporation vessel and transitioning into a gaseous state. Subsequently, it traverses into the falling film evaporation/external condensation vessel via gas valves V3 and V4. Within this vessel, the gaseous refrigerant dispenses its heat to the cold water circulating within the test copper tube, thus undergoing condensation back into a liquid state. The condensed refrigerant is then redirected to the full liquid evaporation vessel through liquid valve V7, effectively concluding a single refrigerant cycle.

## 3. Calculation and Analysis

The experimental focus encompasses the determination of the total heat transfer coefficient of the heat exchange tube, alongside the distinct examination of the heat transfer coefficients both inside and outside the tube.

1) Overall Heat Transfer Coefficient

Given the fluctuating inlet and outlet water temperatures of the test tube, the logarithmic average temperature difference is employed for calculation purposes. The formula for determining the total heat transfer coefficient is as follows:

$$U_0 = \frac{Q}{A_0 \Delta t} \tag{1}$$

$Q$ - Heat Transfer.

$A_0$ - External Surface Area of Heat Transfer Tube.

$\Delta t$ - Logarithmic Mean Temperature Difference.

2) Heat Transfer Coefficient Inside the Tube

The author uses the Sieder-Tate equation[2] to calculate the heat transfer coefficient inside the tube:

$$\mathrm{h}_i = St_i \frac{\lambda}{D_{in}} \mathrm{Re}^{0.8} \mathrm{Pr}^{1/3} \left( \frac{\mu}{\mu_W} \right)^{0.14} \tag{2}$$

$St_i$ - Stanton Number, St.

$\lambda$ - Thermal Conductivity of Fluid Inside Tube.

$D_{in}$ - Nominal Diameter of Inside Tube.

$Re$ - Reynolds Number for Fluid Inside Tube.

$Pr$ - Prandtl Number for Fluid Inside Tube.

$\mu$ - Dynamic Viscosity of Fluid at Mean Temperature.

$\mu_W$ - Dynamic Viscosity of Fluid at Wall Temperature.

Establishing equations based on Wilson's graphical method[3]:

$$\frac{1}{U_0} = \frac{1}{\mathrm{h}_0} + r_s + r_W + \frac{1}{\mathrm{h}_i} \tag{3}$$

As the refrigerant state remains constant, the heat transfer coefficient outside the tube remains consistent. Consequently, variations in the total heat transfer coefficient stem solely from changes in the heat transfer coefficient inside the tube. Given that the test tube is newly fabricated from copper,

ISSN: 2414-1895 DOI: 10.6919/ICJE.202405_10(5).0065

the thermal resistance due to fouling can be disregarded. From the aforementioned formula, it is deduced that:

$$\frac{1}{U_0} = \frac{1}{St} \bullet \frac{1}{\frac{\lambda}{D_{in}} \mathrm{Re}^{0.8} \mathrm{Pr}^{1/3} \left( \frac{\mu}{\mu_W} \right)^{0.14}} + Cons \tag{4}$$

By fitting with the least squares method, the slope of the line is obtained, which is the reciprocal of $s_t$.

3) Heat Transfer Coefficient Inside the Tube

Given the intricate external geometric configurations of surface-enhanced heat transfer tubes, the derivation of a universally applicable and highly precise criterion equation remains a challenge. Consequently, the author opts to employ the following relationship equation:

$$\ln h_0 = \ln F + D \ln q \tag{5}$$

$q$- Heat Flux.

$h_0$- External Heat Transfer Coefficient.

$F$、$D$- Coefficient.

## 4. Conclusion

he heat exchange tube chosen for experimentation is a standard light tube of universal specifications, facilitating straightforward horizontal data comparison. Relevant parameters are detailed in the accompanying table:

**Table 1.** Tube parameters

| Tube Type | Outer Diameter/mm | Inner Diameter/mm | Length/mm |
|---|---|---|---|
| Optical Tube | 25.4 | 23.0 | 2500 |

A 25mm light tube is chosen for conducting full liquid evaporation and external condensation experiments, with subsequent comparison of calculated results against theoretical predictions. It is anticipated that the deviation of the heat transfer coefficient inside the light tube from the Gnielinski model[4] will fall within ± 20%, while deviations from theoretical values proposed by Blasius or McAdams[5] are expected to be within ± 10%. Similarly, the discrepancy between the external film condensation heat transfer coefficient of the light tube and the Nusselt theoretical value is projected to be within ±10%.

A comparative analysis is conducted between the heat transfer coefficient acquired from the full liquid evaporation test and the theoretical values computed using the Gnielinski and McAdams formulas, as illustrated in Figure 4. The results indicate a maximum deviation of 3.1% and a minimum deviation of 9.2% between the experimental data and the theoretical calculations based on the Gnielinski formula, while aligning closely with the theoretical predictions derived from the McAdams formula. Figures 5. and Figures 6. further reveal that, during the external condensation phase, the deviation between the heat transfer coefficient within the light tube and the Gnielinski theoretical value remains marginal. Meanwhile, deviations from the McAdams theoretical calculations range from 10% to 15%. Under high heat flux conditions, the deviation between the heat transfer coefficient

ISSN: 2414-1895 DOI: 10.6919/ICJE.202405_10(5).0065

outside the light tube and the theoretical calculations based on the Nusselt1 formula ranges from 2% to 7%, with a maximum deviation of 7% observed for the theoretical predictions derived from the Nusselt2 formula under low heat flux conditions.

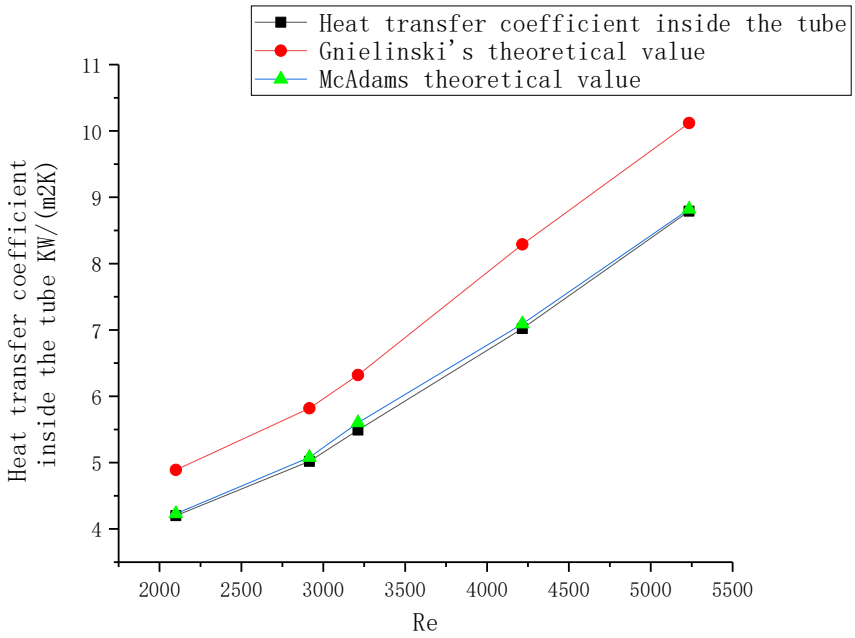


**Figure 4.** Comparison between the Heat Transfer Coefficient and Theoretical Values inside a Full Liquid Vaporized Light Emitting Tube

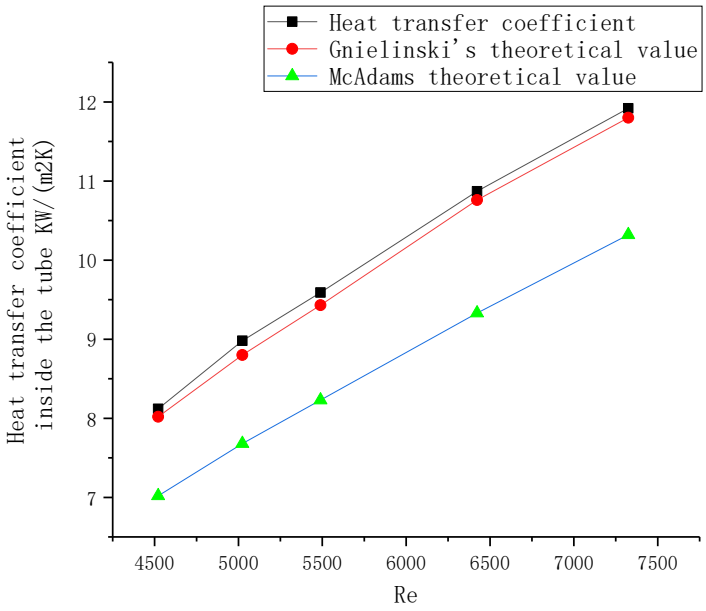


**Figure 5.** Comparison between the heat transfer coefficient and theoretical values inside the condensing light tube outside the tube

The experimental findings demonstrate that modifying the experimental bench structure and transitioning the heat source for external condensation from electric heating within the evaporator vessel to hot water within the evaporator tube contribute to enhanced accuracy in both full liquid

ISSN: 2414-1895 DOI: 10.6919/ICJE.202405_10(5).0065

evaporation and external condensation processes. These modifications not only streamline the experimental procedure but also reduce overall time consumption.

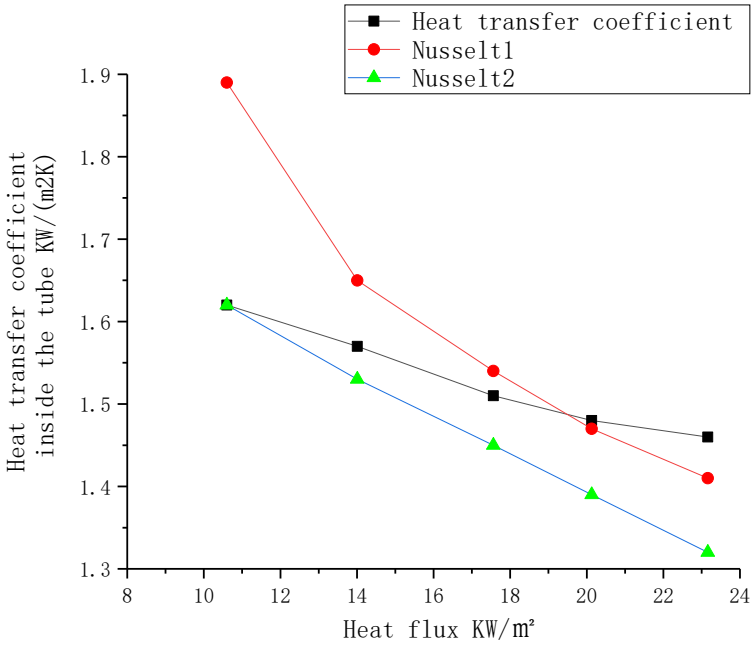


**Figure 6.** Comparison between the External Heat Transfer Coefficient and Theoretical Values of the Condensing Light Tube Outside the Tube

## References

[1] Cui Chao, Weng Wenbing, Liu Yang. Design of test stand for heat transfer performance of horizontal single-tube and its experimental study[J]. Refrigeration and air-conditioning, 2014, 14(04): 126-130.

[2] Luo Zhong, Wu Xiaoyu, Li Wei. Experimental study on water falling film evaporation on enhances tubes[J]. Journal of Engineering Thermophysics, 2010, 31(11): 1893-1896.

[3] Thoo K K, Chin W M, Heikal M R. Determination of air side heat transfer coefficient in a mini-channel heat exchanger using Wilson Plot method[J]. Iop Conference, 2013, 50: 012024.

[4] Ji Wen Tao, Zhang Ding Cai, He Ya Ling, et. Prediction of fully developed turbulent heat transfer of internal helically ribbed tubes - An extension of Gnielinski equation[J]. International Journal of Heat & Mass Transfer, 2012, 55(4): 1375-1384.

[5] Cooper M. G. Heat Flow Rates in Saturated Nucleate Pool Boiling-A Wide-Ranging Examination Using Reduced Properties[J]. Advances in Heat Transfer, 1984.